



OPEN

Global impacts of heat and water stress on food production and severe food insecurity

Tom Kompas^{1✉}, Tuong Nhu Che² & R. Quentin Grafton³

In contrast to most integrated assessment models, with limited transparency on damage functions and recursive temporal dynamics, we use a unique large-dimensional computational global climate and trade model, GTAP-DynW, to directly project the possible intertemporal impacts of water and heat stress on global food supply and food security to 2050. The GTAP-DynW model uses GTAP production and trade data for 141 countries and regions, with varying water and heat stress baselines, and results are aggregated into 30 countries/regions and 30 commodity sectors. Blue water stress projections are drawn from WRI source material and a GTAP-Water database to incorporate dynamic changes in water resources and their availability in agricultural production and international trade, thus providing a more general measure for severe food insecurity from water and heat stress damages with global warming. Findings are presented for three representative concentration pathways: RCP4.5-SSP2, RCP8.5-SPP2, and RCP8.5-SSP3 (population growth only for SSPs) and project: (a) substantial declines, as measured by GCal, in global food production of some 6%, 10%, and 14% to 2050 and (b) the number of additional people with severe food insecurity by 2050, correspondingly, increases by 556 million, 935 million, and 1.36 billion compared to the 2020 model baseline.

Keywords Water stress, Climate change, Agricultural productivity, Food security, Irrigation, Computable General Equilibrium (CGE) models

Climate change is a serious threat to food production systems that are highly dependent on water resources and ecosystems, at multiple scales¹. Various regions already suffer from water cycle disruptions due to climate change which include intensification of extreme weather events (e.g., droughts, floods) and groundwater depletion^{2–4}. Critical future risks include heat stress and water stress on global food production and, thus, food security⁵. Climate change risks are magnified by increasing water withdrawals for household and industry to 2050⁶, especially for irrigated agriculture that accounts for about 70% of total water withdrawals, and supplies up to 40% of the global human-consumed calories⁷.

How these risks are realized, when and where, is determined by domestic and international input–output interactions across commodity sectors and regions, and endowments such as capital, labor, land, natural resources, and water, and the interlinkages of international trade. To quantitatively assess these risks for global food production and food security requires a Computable General Equilibrium (CGE) model, connected to a climate change model, to capture price, trade, and income effects in relation to both food supply and demand.

Previous integrated assessment model (IAM) studies simulating the Shared Socioeconomic Pathways (SSPs) find that changes in population growth and dietary makeup, as well as agricultural efficiencies, lead to increased food insecurity under SSP3 and SSP4⁸. Further, mitigation efforts aimed at lowering land-based emissions have the effect of increasing the cost of production and consequently food prices, particularly within low-income regions^{9,10}. Consequently, SSP top-down results need additional variants to account for inequity in food availability and accessibility¹¹.

In contrast to the vast majority of extant IAM studies that employ coupled-model frameworks with recursive temporal dynamics and with limited transparency about damage functions, our analysis circumvents the need for model coupling through the incorporation of climate change damages and agricultural dynamics, such as changes in irrigation, directly into the core model. In conjunction with intertemporal dynamics, our approach allows for

¹Centre of Excellence for Biosecurity Risk Analysis and the Centre for Environmental and Economic Research, School of Agriculture, Food and Ecosystem Sciences, Faculty of Science, University of Melbourne, Melbourne, Australia. ²Global Environmental and Economic Modelling, Canberra, Australia. ³Crawford School of Public Policy, Australian National University, Canberra, Australia. ✉email: Tom.Kompas@unimelb.edu.au

the simulation of feedbacks directly into the model solution with optimization taking place across all time steps simultaneously.¹² Further, the current study implements a wider range of climate change damages on factors of production, such as the impact of heat stress on labor productivity, which is frequently missing within IAM.

We used a unique intertemporal CGE model, GTAP-DynW, that extends the GTAP-AEZ, Version 10¹³ platform, and includes the GTAP-Water dataset¹⁴ to project global food production and food security to 2050. GTAP-DynW incorporates dynamic changes in water resources and their availability in agricultural production and international trade and also includes a food security component with climate change damages^{15–17}. Model results are aggregated from 141 countries in GTAP-DynW to 30 countries and/or regions and for 30 commodities to provide global projections.

The scenario framework adopted here is based on SSP quantitative demographic data¹⁸ from the SSP2 and SSP3 scenarios as well as temperature pathways associated with the Representative Concentration Pathway (RCP) RCP4.5 and RCP8.5. Note that the current model does not directly encompass emissions and, therefore, combinations deemed infeasible within a standard SSP-RCP framework (e.g., SSP2-RCP8.5) are a potential future outcome due to uncertainties regarding feedbacks, and climate sensitivity^{19,20}. For each of the three reported projections, we used the same population projection for each SSP (2,3) and ensured the temperature pathways in our model were consistent with the given RCP (4.5, 8.5). We assumed that the RCP8.5 scenario to 2100 remains useful in terms of model runs which use a mid-century time horizon²¹.

The impacts of water and heat stress from climate change on agricultural production and food security to 2050 were quantified using GTAP-DynW for three SSP population (only)/temperature combinations, SSP2-RCP4.5, SSP2-RCP8.5, and SSP3-RCP8.5 for decadal projections to 2050. These combinations are consistent with the WRI and GTAP databases. Impacts on individual agricultural commodities (e.g., paddy rice, wheat, etc.) from both irrigated and non-irrigated agriculture were summarized as GCal measures of global food production by country/region²² relative to 2020. Estimates of the additional people by 2050, relative to 2020, who could be classified with severe food insecurity, as per the Food Insecurity Experience Scale²³, were then calculated by dividing the projected global food supply in GCal by the average per person dietary requirements per year.

Detailed information on the estimates of the heat and water stress damage functions and all relevant source material are given in the Supplementary Information. The initial projections for water stress are at the basin level and estimated as the ratio of water withdrawals to available blue water. Technical detail on model construction of GTAP-DynW is in the "Methods" section below and an illustrative figure of model structure for GTAP-DynW is contained in the Supplementary Information. Note that our projections of water and heat stress apply only to irrigated agriculture. For non-irrigated agriculture we make projections based on heat stress alone.

Results

Model results for SSP2-RCP4.5, SSP2-RCP8.5, and SSP3-RCP8.5, respectively, project: (a) substantial declines, as measured by GCal, in global food production of some 6%, 10%, and 14% to 2050 and (b) the number of additional people with severe food insecurity by 2050, correspondingly, increases by 556 million, 935 million, and 1.36 billion compared to the 2020 model baseline.

Food production

Food production is aggregated as total nutrition by thousand Giga-calories (thous. GCal) by region and million Gcal for the world using nutritional conversion factors for the total production of food across all food commodity sectors. A decrease in agricultural output causes a reduction in global food production (measured in total energy for nutrition) that, in turn, increases the number of people (millions) with severe food insecurity. GTAP-DynW provides these measures as model output for all climate change scenarios.

Figure 1a–c shows a decreasing trend of food production as a % reduction in 2050 from 2020 for each climate change scenario. Global food production falls by 5.8%, 9.7%, and 14.2%, on average, for the scenarios SSP2-RCP4.5, SSP2-RCP8.5, and SSP3-RCP8.5, respectively. Globally, for scenarios SSP2-RCP4.5, SSP2-RCP8.5, and SSP3-RCP8.5, food production decreases from 9.75 million to 9.2, 8.8, and 8.4 million GCal, respectively by 2050.

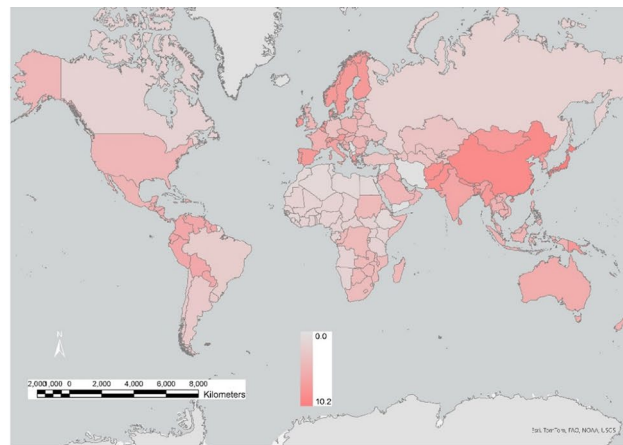
For SSP2-RCP4.5 the food production from both water and heat stress is projected to fall by 5.1–6.6% in Africa, 5.8% in Australia, and 6.4% for some parts of South America. In 2050, food production is projected to fall by 4.8% for the USA, 9.0% for China, and 6.5% for India. For SSP3-RCP8.5, the worst-case scenario, food production is projected to decline by 8.2–11.8% in Africa, 14.7% for Australia, and 19.4% for some parts of Central America. For SSP3-RCP8.5, in 2050, global food production is projected to fall by 12.6% for the USA, 22.4% for China, and 16.1% for India.

Food security

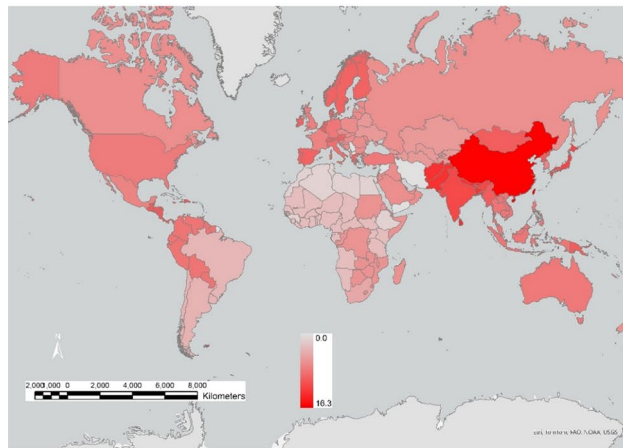
The number of persons (millions) with severe food insecurity caused by a decrease in global food production (or aggregated nutritional supply) is calculated as the reduction in food production relative to base nutritional supply. All outputs are trade-adjusted, noting that for net food exporting countries/regions a fall in their domestically produced food production does not necessarily increase their domestic food insecurity (e.g., Australia, France, Russia and the USA).

Heat stress and water stress from climate change both increase global food insecurity (see Fig. 2a–c). Overall, Africa is the most threatened in terms of severe food insecurity because of reductions in the continent's food production due to water and heat stress and because of the projected increase in Africa's population by 2050. Other regions with substantial increases in severe food insecurity include the Middle East, South Asia, and Central America.

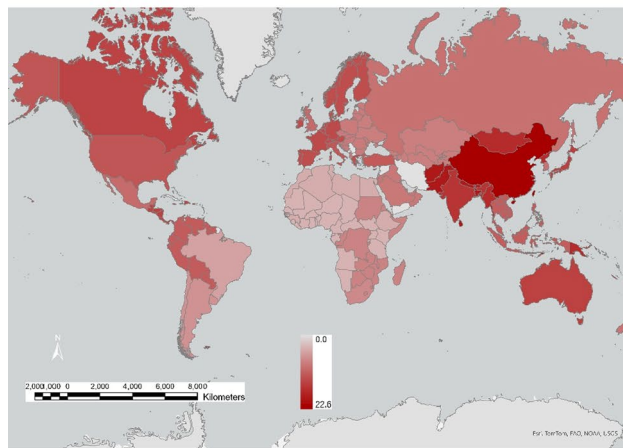
For the SSP3-RCP8.5 case, domestic food production in many African countries will provide less than half of their domestic food demand (Fig. 2c). Some regions, such as China and ASEAN countries, switch from



a) SSP2-RCP4.5



b) SSP2-RCP8.5

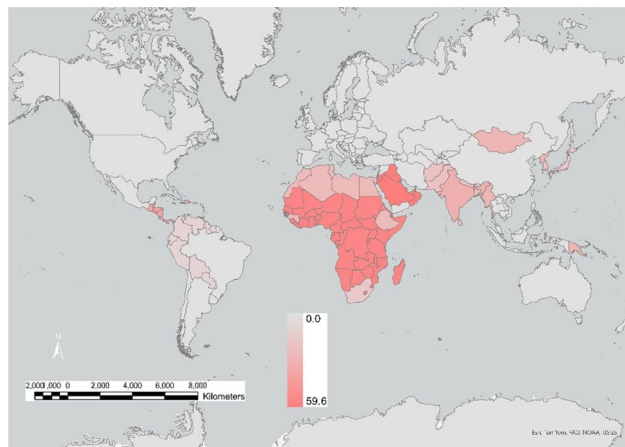


c) SSP3-RCP8.5

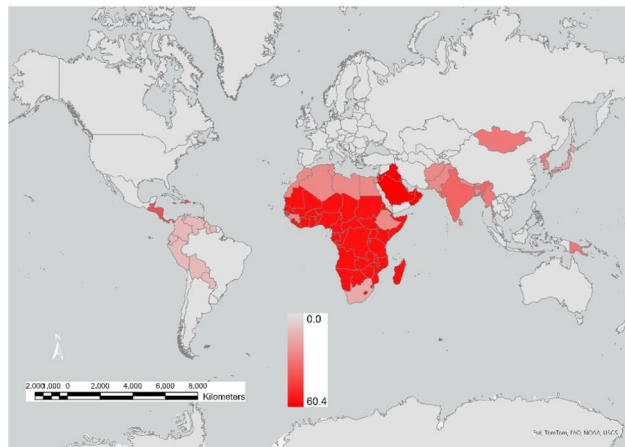
Figure 1. | Regional food production reduction from irrigated agriculture due to heat stress and water stress in 2050 relative to 2020 (% ranges). Model output; maps generated using ArcGIS Pro 3.3 (<https://www.esri.com>).

being net food exporters to food importers by 2050, with a need to import from food-producing regions that are impacted by climate change. Globally, the number of additional people with severe food insecurity by 2050, relative to 2020, for scenarios SSP2-RCP4.5, SSP2-RCP8.5, and SSP3-RCP8.5 are 556 million, 935 million and 1.36 billion, respectively.

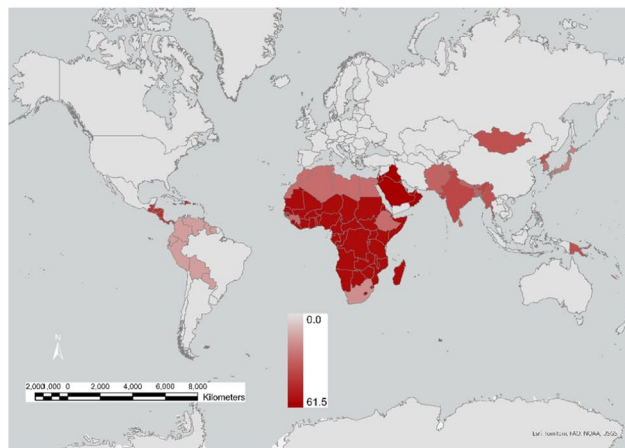
In terms of prices and trade flows (i.e., exports and imports), the projected changes in our large dimensional model are complex, but the general results are robust. In all cases, model results show that there are substantial increases in food prices overall, and especially for the most extreme scenario and for those regions with high



a) SSP2-RCP4.5



b) SSP2-RCP8.5



c) SSP3-RCP8.5

Figure 2. | Persons with severe food insecurity by region in 2050 relative to 2020 (% population range). Model output; maps generated using ArcGIS Pro 3.3 (<https://www.esri.com>).

water stress. Our results show an increased flow of trade in agricultural commodities from low to high water stress countries and regions, given (in part) by the relative regional food price changes. Food exports to China, from lower water stress countries, increase across all three scenarios.

Discussion

Our results highlight the regional and global magnitude of both heat stress and water stress on global food production. The value add of our modeling and projections are that we: (1) quantify both heat and water stress on global food production, noting that irrigation, in general, reduces the risks of water stress on crops relative to non-irrigated land²⁴; (b) account for global commodity price changes (30 commodities) and the reallocation of resources across 30 countries/regions; (3) incorporate trade effects noting that climate change and water withdrawals, especially groundwater depletion, can transmit risks from water-stressed regions to regions without water stress via food trade²⁵; and (4) allow producers and households to be forward-looking.

Climate change has already had a substantial and negative impact on global agricultural productivity, reducing a global measure of agricultural productivity by about 20% since 1970, with larger negative impacts in the Near East and North Africa²⁶. Adverse impacts on productivity and yields will magnify with future climate change given longer duration, higher magnitude, and more frequent heat extremes²⁷ and droughts^{28,29}. To what extent technological change can offset yield declines from climate change is uncertain^{30–33}. Future water availability for increased food production is also uncertain as the irrigated area in water-stressed regions is increasing, including in major food-producing regions such as China, India, Pakistan and the United State. In part, this is because the area in irrigation drives irrigated water withdrawals in these countries and because climate change will likely increase crop demand by further expanding irrigation^{34–36}.

Global studies of the decline in terrestrial water storage^{37,38} show statistically significant declines in global storages over the period 1992–2020 in about half of all 1058 natural lakes and 922 global reservoirs. Over half of the decline in the storages is attributable to water withdrawals, increasing temperatures and potential evapotranspiration⁴. The OECD⁷ highlights that water stress, in the absence of effective policy actions in terms of water management, will significantly and negatively impact agricultural production in Northeast China, Northwest India and Southwest United States. These locations are in the world's three largest food producing countries, all of which are currently net food exporters and have the biggest cumulative food footprints³⁹. Other modeling in the existing literature highlight that the frequency of crop yield failures with climate change could be many times greater for key cereal crops (rice, soybean, maize, and wheat) that account for about two-thirds of food calorie consumption⁴⁰ for China, India, and the USA over the period 2041–2060⁴¹.

A key limitation in our study is that results, using the WRI index, are based only on blue water (irrigation) sources. Water stress impacts on rainfed croplands are not yet available for use in our GTAP framework. Although we do include the impacts of heat stress on agriculture generally, it is important to recognize that rainfed croplands will not be impacted by heat stress only. Climate change alters precipitation patterns, thus modifying the spatial and temporal distribution of green water availability for both rainfed croplands and irrigated crops. While a shift from blue to green water crops can potentially and partially offset food production losses from heat and water stress in irrigated agriculture⁴², both blue water⁴³ and green water⁴⁴, globally, are under threat, especially in South Asia, East Asia, and the Middle East. Consequently, increases in agricultural production in either irrigated or rainfed agriculture in water-stressed regions will likely be at the expense of further groundwater depletion, inadequate stream flows and/or biodiversity loss. Agricultural extensification and increased rainfed cropping may pose additional sustainability challenges; over the period 2003–2019, about half of the 9% global increase in the cropland area removed natural vegetation and tree cover⁴⁵.

Our results highlight the critical importance of quantifying the trade-offs in relation to water and food⁴⁶ and climate change⁴⁷. Food systems already contribute about one-third of anthropogenic greenhouse gas emissions⁴⁸ and emissions from food production and consumption alone could contribute, under SSP2-RCP4.5, to almost a 1°C increase in the global surface temperature by 2100⁴⁹. Food systems are also major contributors to biodiversity loss in Central and South America, and Africa⁵⁰.

A major challenge is to increase regional and global food production without contributing to further climate change or increased water stress⁵¹, while ensuring sustainability^{52,53}. This requires nothing less than a transformation in the world food systems^{54–56} simultaneous with much greater reductions in current greenhouse gas emissions from all sources, including agriculture.

Methods

The GTAP-DynW model is a large dimensional CGE model that uses the extensive GTAP (Global Trade Analysis Project) Data Base Version 10⁵⁷ in which countries or regions interact, importing goods and services from each other. GTAP-DynW is a (forward-looking) intertemporal rather than a recursive CGE model and includes 18 Agro-Economic Zones⁵⁸ to characterize climate, soil, and terrain conditions pertinent to agricultural production⁵⁹. Following Kompas and Van Ha¹⁶ and Kompas et al.¹⁵, the model also includes climate change damage functions.

In GTAP-DynW, within each country or region, a producer combines inputs (land, labor, capital, an intermediate good, and natural resources) to produce a single good or service, which is consumed domestically by regional households (i.e., final consumption) and producers (i.e., intermediate demand for products as inputs in the production of other commodities) or is exported to other international or regional households and producers. Producers account for future impacts and policy settings as per the following system of motion equations:

$$\dot{k}_{r,t} = \varphi_{r,t} - \delta_r k_{r,t} \quad (1)$$

$$\dot{\mu}_{r,t} = \mu_{r,t}[\dot{i}_t + \delta_r] - \frac{\phi_r}{2} \left(\frac{\psi_r}{k_{r,t}} \right)^2 p_{r,t}^I - p_{r,t}^K \quad (2)$$

where $p_{r,t}^K$ and $k_{r,t}$ are the rental price of capital and the capital stock in region r at time t ; $p_{r,t}^I$ is price of an investment good; δ_r is the capital depreciation rate; ψ_r is the capital increment from the (gross) investment activity; i_r is the global interest rate; ϕ_r is an investment increment coefficient; and $\mu_{r,t}$ is the shadow price of capital.

Water stress effects

The production of agriculture output ($Q_{i,t}$) is approximated by a constant elasticity substitution (CES) production function that includes the demand for commodity i for use by j ($QF_{i,j,t}$) from both domestic and imported sources, and the value added in the industry j ($QVA_{j,t}$). The demand of endowments ($QSE_{i,j,t}$) that includes the 18 AEZ land use categories and natural resources for the value added in the industry j ($QVA_{j,t}$) is given by:

$$QSE_{i,j,t} = \left[\frac{QVA_{j,t}}{afe_{i,j,t}} \right] \left(\frac{afe_{i,j,t}}{PSE_{i,j,t}} \frac{PVA_{j,t}}{PSE_{i,j,t}} \right)^{\gamma_{j,t}} \quad (3)$$

where $afe_{i,j,t}$ is augmenting technological change of the endowments i by j ; $PSE_{i,j,t}$ is the market price of 'sluggish' endowment i (e.g., land which is hard to reallocate) used by industry j ; $PVA_{j,t}$ is the firm's price of value added in industry j ; and $\gamma_{j,t}$ is the elasticity of transformation for sluggish primary factor endowments in the production of value-added in j .

Under the effect of water and heat stress, with climate change, the effectiveness of land use for agriculture or AEZ land decreases, where the relative reduction in the efficiency of land endowments is directly proportional to the relative increase in water stress. In GTAP-DynW, water stresses are derived from WRI⁶⁰. This global GIS water data of 15,006 basins was spatially merged with the global GIS layers Esri-USGS⁶¹ to generate a geographical water stress projection for 174 countries, and then mapped to accord with GTAP-DynW's 30 aggregate countries/regions. Water stress at a time by a region i is estimated from the projection of water stress in all basins j located in the region i with a weighted coefficient of j that is measured as the area or share of j in the total basin area in i , or

$$ws(i) = \sum_{j=1}^J wsb(i,j) \frac{B(i,j)}{\sum_{j=1}^J B(i,j)} \quad (4)$$

where $wsb(i,j)$ is the water stress of a basin j (in the set of J basins located in region i), i belongs to the GTAP-DynW's 30 regions (I); and $B(i,j)$ is the area of basin j located in i .

Water stress affects land use by AEZ by region and time in $QFE_{i,j,t}$ and changes $QVA_{j,t}$ and, thus, agricultural production ($Q_{i,t}$). The water stress indicators are deviations (i.e., too much and too little) from the 2020 baseline under the effect of climate change, following WRI⁶⁰, and are quantified only for irrigated agriculture. The magnitudes of the water stress shock by AEZ depends on the share of irrigated land in total land use in the region's AEZ ($w_{c,irr}$) and the change of irrigated water volume in that AEZ in a region ($dIW_{c,t}$), is given by:

$$QSE_{i,j,t} = \frac{\overbrace{L(c, irr)}^{w_{c,irr}}}{L(c)} dIW_{c,t} \quad (5)$$

where c, j, t represents 18 AEZ land types, agricultural commodity, and time.

To calibrate the impact of water stress on agricultural outputs, we assumed a constant elasticity of substitution (CES) production function and defined demands for intermediate inputs ($QF_{i,j,t}$) by:

$$QF_{i,j,t} = \left[A_{i,j,t} \frac{Q_{j,t}}{afw2_{j,t} \left(\frac{pf_{i,j,t}}{afw1_{i,t}} \frac{1}{ps_{j,t}} \right)^{\gamma_{j,t}}} \right] \quad (6)$$

where $Q_{j,t}$ is the agricultural output of commodity j ; $pf_{i,j,t}$ is the firm's price for input commodity i for use by j ; $ps_{j,t}$ is the supply price of commodity j ; $A_{i,j,t}$ is the composite regional variable of augmenting technology change; and $\gamma_{j,t}$ is the elasticity of substitution among composite intermediate inputs in the agricultural sector j . Two specific augmenting technology change variables include a water stress factor ($afw1_{i,t}$) for intermediate inputs and endowments used for production, and a region-specific average rate of intermediates augmenting technology change of j ($afw2_{j,t}$).

The shock $afw1_{c,j,t}$ depends on the weighted coefficient of irrigated land in total land use for an agricultural crop $w_{irr,j}$, the change of irrigated water by time ($dIW_{c,t}$), and the water stress coefficient to crop yields, or

$$dafw1_{c,j,t} = \frac{\overbrace{L(c, irr)}^{w_{irr,j}}}{L(c,j)} \frac{1}{dIW_{c,t}} ws_{c,j,t} \quad (7)$$

where c, j, t represents 18 AEZ land types, agricultural commodity, and time. Water prices from water resources paid by water user industries are added to regional income, but also increase costs in these sectors that may cause a shift or reallocation of water use among water using industries. For a water price $p_{water}(t)$ in a region r , the price index for purchases of k commodity by j sector in region r ($PFE_{j,k,r,t}$) is given by:

$$PFE_{k,j,r,t} = [p_{k,j,r,t} + taxF_{k,j,t}] + \left(\frac{pwater_{r,t} * WIN_{j,k,r,t}}{VFA_{k,j,r,t}} \right) \quad (8)$$

where $VFA_{j,k,r,t}$ is the purchase and firm's tax of k inputs for use by sector j ; $p_{j,k,r,t}$ is the market price of k to j ; $taxF_{j,k,r,t}$ is the tax on firm's purchases of k by production j ; $pwater_{r,t}$ is water price at t ; and $WIN_{j,k,r,t}$ is the water intensity of j on k . Thus, a water stress shock causes a change in $PFE_{j,k,r,t}$ and a shift in water withdrawals from domestic and imported sources depends on the domestic and import commodity mix.

Heat stress effects

Damage functions provide the relationships between climate variables (such as average temperature, humidity, or extreme heat days) on productivity, income, and resource endowments⁶². Roson and Sartori⁶² provide the estimated parameters of damage functions for 120 GTAP countries and regions using GTAP9 with six climate impacts: sea level rise, variation in crop yields, heat stress effects on labor productivity, human health, tourism, and household energy demand. Projections from GTAP-DynW include damage functions related to heat stress and their impacts on agricultural outputs and labor productivity in the agricultural sector using GTAP10a. The heat stress shocks from global warming (e.g. losses in agricultural and labor productivity) are based on Kompas et al.¹⁵, Kompas and Van Ha¹⁶, and Roson and Sartori⁶².

Food security effects

In GTAP-DynW, each food commodity contains nutritional components with different energy intake (calories). The aggregated nutritional supply in the region r ($S(r, t)$) (measured as Giga-calories (GCal)) is aggregated as a sum of nutritional supply from food production i or

$$S(r, t) = \sum_{i=1}^I \frac{S(i, r, t)z(i) * 1000}{10^9} \quad (9)$$

where $S(i, r, t)$ is food production i (thousand tons); and $z(i)$ is the nutrition conversion factors of food i for calculating that food's energy content from one ton of food i to calories. The average daily nutrition intake a required for human food security is taken as given, and varies by country and region (source data: FAO^{22,63,64}) and is given by:

$$F(r, t) = \frac{S(r, t) * 10^9}{a * 365 * 10^6} \quad (10)$$

where a is average daily nutrition in calories. Global food production (GCal) is the sum of all regional food supply and the total population across regions is $F(r, t)$.

The number of persons with severe food insecurity, in millions, is determined by the gap in the minimum calorie demand and the available production and is given by:

$$IF(r, t) = \frac{\overbrace{[S(r, 0) - S(r, t)]}^{ds(r, t)} * 10^9}{a * 365 * 10^6} \quad (11)$$

where $ds(r, t)$ is the reduction of food production in region r at t to the base nutritional supply ($S(r, 0)$).

The food insecurity rate ($RIF(r, t)$) is the ratio of the number of persons with severe food insecurity over the total population of that country or $POP(r, t)$:

$$RIF(r, t) = \frac{IF(r, t)}{POP(r, t)} \quad (12)$$

The global reduction of food production ($ds(t)$) is the sum of the reduction of food supply ($ds(r, t)$) across all regions. The global number of persons with severe food insecurity ($IF(t)$) is the sum of all regions' persons with severe food insecurity resulting from the reduction of food supply (or $IF(r, t)$).

Data availability

Model code and data sources available at: <https://doi.org/10.5281/zenodo.8248417>

Received: 27 November 2023; Accepted: 18 June 2024

Published online: 22 June 2024

References

1. Sivakumar, B. Global climate change and its impacts on water resources planning and management: assessment and challenges. *Stoch. Env. Res. Risk Assess.* **25**, 583–600 (2011).
2. Fecht, S. How climate change impacts our water. *Columbia Climate School Climate, Earth and Society* <https://news.climate.columbia.edu/2019/09/23/climate-change-impacts-water/> (2019).
3. Scanlon, B. R. et al. Global water resources and the role of groundwater in a resilient water future. *Nat. Rev. Earth Environ.* **4**, 87–101 (2023).
4. Yao, F. et al. Satellites reveal widespread decline in global lake water storage. *Science* **380**, 743–749 (2023).
5. Zolin, C. A. & de Rodrigues, R. A. R. *Impact of Climate Change on Water Resources in Agriculture* (CRC Press, Boca Raton, 2015).
6. Luck, M., Landis, M. & Gassert, F. Aqueduct water stress projections: Decadal projections of water supply and demand using CMIP5 GCMs. *Washington, DC* (2015).

7. Co-Operation, O. for E. & Development (OECD). *The Land-Water-Energy Nexus: Biophysical and Economic Consequences*. (IWA Publishing, 2017).
8. Doelman, J. C. *et al.* Exploring SSP land-use dynamics using the IMAGE model: Regional and gridded scenarios of land-use change and land-based climate change mitigation. *Global Environ. Change* **48**, 119–135 (2018).
9. Fujimori, S. *et al.* A multi-model assessment of food security implications of climate change mitigation. *Nat. Sustain.* **2**, 386–396 (2019).
10. Hasegawa, T. *et al.* Risk of increased food insecurity under stringent global climate change mitigation policy. *Nature Climate Change* **8**, 699–703 (2018).
11. Van Meijl, H. *et al.* Modelling alternative futures of global food security: Insights from FOODSECURE. *Global Food Secur.* **25**, 100358 (2020).
12. Babiker, M., Gurgel, A., Paltsev, S. & Reilly, J. Forward-looking versus recursive-dynamic modeling in climate policy analysis: A comparison. *Econ. Model.* **26**, 1341–1354 (2009).
13. Plevin, R., Gibbs, H., Duffy, J., Yui, S. & Yeh, S. *Agro-Ecological Zone Emission Factor (AEZ-EF) Model (V47)*. (2014).
14. Haqiqi, I., Taheripour, F., Liu, J. & van der Mensbrugghe, D. Introducing irrigation water into GTAP Data Base Version 9. *J. Global Econ. Anal.* **1**, 116–155 (2016).
15. Kompas, T., Pham, V. H. & Che, T. N. The effects of climate change on GDP by country and the global economic gains from complying with the Paris Climate Accord. *Earth's Future* **6**, 1153–1173 (2018).
16. Kompas, T. & Ha, P. V. The 'curse of dimensionality' resolved: The effects of climate change and trade barriers in large dimensional modelling. *Econ. Model.* **80**, 103–110 (2019).
17. Piontek, F. *et al.* Integrated perspective on translating biophysical to economic impacts of climate change. *Nat. Climate Change* **11**, 563–572 (2021).
18. Kc, S. & Lutz, W. The human core of the shared socioeconomic pathways: Population scenarios by age, sex and level of education for all countries to 2100. *Global Environ Change* **42**, 181–192 (2017).
19. Lenton, T. M. & Williams, H. T. On the origin of planetary-scale tipping points. *Trends Ecol Evol* **28**, 380–382 (2013).
20. Sherwood, S. C. *et al.* An assessment of Earth's climate sensitivity using multiple lines of evidence. *Rev Geophys* **58**, e2019RG000678 (2020).
21. Schwalm, C. R., Glendon, S. & Duffy, P. B. RCP8.5 tracks cumulative CO₂ emissions. *Proc. Natl. Acad. Sci. U.S.A.* **117**, 19656–19657 (2020).
22. FAO. 'FAO Statistics', Food and Agriculture Organization of the United Nations. (2022).
23. FAO. The Food Insecurity Experience Scale: Measuring food insecurity through people's experiences. (2017).
24. Giordano, M., Namara, R. & Bassini, E. *The impacts of irrigation: a review of published evidence* (Washington, DC, USA, The World Bank, 2019).
25. Dolan, F. *et al.* Evaluating the economic impact of water scarcity in a changing world. *Nat. Commun.* **12**, 1–10 (2021).
26. Ortiz-Bobea, A., Ault, T. R., Carrillo, C. M., Chambers, R. G. & Lobell, D. B. Anthropogenic climate change has slowed global agricultural productivity growth. *Nat. Climate Change* **11**, 306–312 (2021).
27. Moore, F. C., Baldos, U., Hertel, T. & Diaz, D. New science of climate change impacts on agriculture implies higher social cost of carbon. *Nat. Commun.* **8**, 1607 (2017).
28. Santini, M., Noce, S., Antonelli, M. & Caporaso, L. Complex drought patterns robustly explain global yield loss for major crops. *Sci. Rep.* **12**, 5792 (2022).
29. Vicente-Serrano, S. M. *et al.* Global drought trends and future projections. *Philos. Trans. Royal Soc. A* **380**, 20210285 (2022).
30. Asseng, S. *et al.* Rising temperatures reduce global wheat production. *Nat. Climate Change* **5**, 143–147 (2015).
31. Iizumi, T. & Sakai, T. The global dataset of historical yields for major crops 1981–2016. *Sci. Data* **7**, 97 (2020).
32. Lobell, D. B. & Field, C. B. Global scale climate–crop yield relationships and the impacts of recent warming. *Environ. Res. Lett.* **2**, 014002 (2007).
33. McLachlan, B. A., Van Kooten, G. C. & Zheng, Z. Country-level climate–crop yield relationships and the impacts of climate change on food security. *SN Appl. Sci.* **2**, 1650 (2020).
34. Mehta, P. *et al.* Half of twenty-first century global irrigation expansion has been in water-stressed regions. *Nature Water* **2**, 1–8 (2024).
35. Puy, A., Borgonovo, E., Lo Piano, S., Levin, S. A. & Saltelli, A. Irrigated areas drive irrigation water withdrawals. *Nat. Commun.* **12**, 4525 (2021).
36. Bhattarai, N. *et al.* Warming temperatures exacerbate groundwater depletion rates in India. *Sci. Adv.* **9**, eadi1401 (2023).
37. Pokhrel, Y. *et al.* Global terrestrial water storage and drought severity under climate change. *Nat. Climate Change* **11**, 226–233 (2021).
38. Wada, Y. *et al.* Global depletion of groundwater resources. *Geophys. Res. Lett.* **37**, 20 (2010).
39. Halpern, B. S. *et al.* The environmental footprint of global food production. *Nat. Sustain.* **5**, 1027–1039 (2022).
40. Kim, W., Iizumi, T. & Nishimori, M. Global patterns of crop production losses associated with droughts from 1983 to 2009. *J. Appl. Meteorol. Climatol.* **58**, 1233–1244 (2019).
41. Caparas, M., Zobel, Z., Castanho, A. D. & Schwalm, C. R. Increasing risks of crop failure and water scarcity in global breadbaskets by 2030. *Environ. Res. Lett.* **16**, 104013 (2021).
42. HLPE. *Water for Food Security and Nutrition*. (High Level Panel of Experts on Food Security and Nutrition of the Committee on World Food Security, Italy, 2015).
43. Rosa, L., Chiarelli, D. D., Rulli, M. C., Dell'Angelo, J. & D'Odorico, P. Global agricultural economic water scarcity. *Sci. Adv.* **6**, eaaz6031 (2020).
44. Schyns, J. F., Hoekstra, A. Y., Booij, M. J., Hogeboom, R. J. & Mekonnen, M. M. Limits to the world's green water resources for food, feed, fiber, timber, and bioenergy. *Proc. Nat. Acad. Sci.* **116**, 4893–4898 (2019).
45. Potapov, P. *et al.* Global maps of cropland extent and change show accelerated cropland expansion in the twenty-first century. *Nat. Food* **3**, 19–28 (2022).
46. Grafton, R. Q., Williams, J. & Jiang, Q. Possible pathways and tensions in the food and water nexus. *Earth's Future* **5**, 449–462 (2017).
47. Grafton, R. Q. *et al.* Global insights into water resources, climate change and governance. *Nat. Climate Change* **3**, 315–321 (2013).
48. Crippa, M. *et al.* Food systems are responsible for a third of global anthropogenic GHG emissions. *Nat. Food* **2**, 198–209 (2021).
49. Ivanovich, C. C., Sun, T., Gordon, D. R. & Ocko, I. B. Future warming from global food consumption. *Nat. Climate Change* **13**, 297–302 (2023).
50. Marques, A. *et al.* Increasing impacts of land use on biodiversity and carbon sequestration driven by population and economic growth. *Nat. Ecol. Evol.* **3**, 628–637 (2019).
51. Grafton, R. Q. *et al.* Water planning and hydro-climatic change in the Murray-Darling Basin Australia. *Ambio* **43**, 1082–1092 (2014).
52. Béné, C. *et al.* When food systems meet sustainability—Current narratives and implications for actions. *World Dev.* **113**, 116–130 (2019).
53. Prutzer, E. *et al.* Climate-smart irrigation and responsible innovation in South Asia: A systematic mapping. *Ambio* **52**, 2009–2022 (2023).

54. FAO. *How to Feed the World in 2050*. https://www.fao.org/fileadmin/templates/wsfs/docs/expert_paper/How_to_Feed_the_World_in_2050.pdf (2015).
55. Fischer, G., Tubiello, F. N., Van Velthuis, H. & Wiberg, D. A. Climate change impacts on irrigation water requirements: Effects of mitigation, 1990–2080. *Technol. Forecasting Social Change* **74**, 1083–1107 (2007).
56. Ringler, C. *et al.* The role of water in transforming food systems. *Global Food Secur.* **33**, 100639 (2022).
57. Aguiar, A., Chepeliev, M., Corong, E. & McDougall, R. The GTAP Data base: Version 10. *J. Global Econ. Anal.* **4**, 27 (2019).
58. Lee, H.-L. Incorporating Agro-Ecologically Zoned Land Use Data and Land-based Greenhouse Gases Emissions into the GTAP Framework. in *8th Annual Conference on Global Economic Analysis* 35 (Citeseer, Lübeck, Germany, 2005).
59. Lee, H.-L., Hertel, T. W. & Rose, S. An integrated global land use database for CGE analysis of climate policy options. In *Economic Analysis of Land Use in Global Climate Change Policy* 92–108 (Routledge, London, 2009).
60. WRI. *Aqueduct Water Stress Projections*. (2022).
61. ESRI-USGS. 'ArcGIS Data Store', ArcGIS Enterprise.
62. Roson, R. & Sartori, M. Estimation of climate change damage functions for 140 regions in the GTAP 9 database. *J. Global Econ. Anal.* **1**, 78–115 (2016).
63. FAO. Average daily dietary energy consumption per capita. (2020).
64. FAO. Calculation of the energy contents of foods-energy conversion factors. (2020).

Author contributions

T.K. and Q.G. conceived the idea, helped with the analysis and helped prepare the manuscript. T.N.C. helped with the analysis, helped prepare the manuscript and prepared all figures. All authors reviewed the manuscript.

Competing interests

The authors declare no competing interests.

Additional information

Supplementary Information The online version contains supplementary material available at <https://doi.org/10.1038/s41598-024-65274-z>.

Correspondence and requests for materials should be addressed to T.K.

Reprints and permissions information is available at www.nature.com/reprints.

Publisher's note Springer Nature remains neutral with regard to jurisdictional claims in published maps and institutional affiliations.



Open Access This article is licensed under a Creative Commons Attribution 4.0 International License, which permits use, sharing, adaptation, distribution and reproduction in any medium or format, as long as you give appropriate credit to the original author(s) and the source, provide a link to the Creative Commons licence, and indicate if changes were made. The images or other third party material in this article are included in the article's Creative Commons licence, unless indicated otherwise in a credit line to the material. If material is not included in the article's Creative Commons licence and your intended use is not permitted by statutory regulation or exceeds the permitted use, you will need to obtain permission directly from the copyright holder. To view a copy of this licence, visit <http://creativecommons.org/licenses/by/4.0/>.

© The Author(s) 2024